DISCRETE SARCOMERE LENGTH DISTRIBUTION IN SKELETAL MUSCLE

T. TAMEYASU, N. ISHIDE, AND G. H. POLLACK
Department of Anesthesiology and Division of Bioengineering, University of Washington, RN-10, Seattle, Washington 98195

ABSTRACT We analyzed the microstructure in the first-order laser diffraction line from both resting and tetanically contracting single twitch fibers from frog anterior tibial muscle to see if the distribution of sarcomere lengths is continuous or discrete. Measuring the distance between adjacent microstructural elements lying parallel, we plotted a histogram of the corresponding differences of sarcomere length. The histograms obtained both from resting and contracting fibers had a prominent peak at ~12–14 nm. The result suggests that the sarcomere length distribution may be discrete with unit separation of ~12–14-nm sarcomere length.

INTRODUCTION

Cleworth and Edman (1972) reported that in single frog twitch fibers, each order of the diffraction pattern was composed of many fine lines, or "microstructure". On the hypothesis that each microstructural line comes from a cluster of sarcomeres whose length is homogeneous and whose orientation satisfies the Bragg condition, Rüdel and Zite-Ferenczy (1979) suggested that the microstructural pattern results from small differences of sarcomere length (SL) among the various clusters. This implies that the distribution of SL (at least those detected) may be discrete, not continuous.

Preliminary data from our laboratory showed that the microstructural elements in the first-order diffraction line were separated predominantly by the value that corresponded to ~40–45-nm separation in terms of the SL difference (Iwazumi et al., 1977). Halpern (1978), on the other hand, reported the values of 30 and 50 nm at SL of 2.0–2.4 μm and of 2.7–2.9 μm, respectively.

We studied this phenomenon further with improved resolution. We suggest that the SL distribution is discrete both during the resting and tetanically contracting state, with the unit separation of SL around 12–14 nm.

METHODS

Preparation

Single twitch fibers were dissected from the anterior tibial muscle of the frog (*Rana pipiens*). The fiber was mounted horizontally in a chamber filled with Ringer's solution. Tendinous ends were fixed with stainless-steel wires. Care was taken to avoid torsion of the fiber, which causes a skew of the laser diffraction lines. The Ringer solution (NaCl, 110 mM; KCl 2.0 mM; $CaCl_2$, 1.8 mM; imidazole buffer, 10 mM; pH adjusted to 7.2–7.8) was circulated continuously during the experiments. A glass cover slip (thickness, 0.17 mm) was placed on the surface of the fluid in the chamber to prevent surface vibration. Temperature in the chamber was kept at 10–15°C.

Optical Setup

The fiber was transilluminated from the bottom of the chamber by a He-Ne laser beam (Melles Griot Inc. 10 mW, 1.0 mm Diam, wavelength $\lambda = 0.6328$ μm). The beam diffracted by the fiber was reflected by a 45° front surface mirror, and projected onto a frosted screen. The pattern was photographed with a kymograph camera (model C4-K, Grass Instrument Co., Quincy, Mass.) from the back of the screen at a shutter speed of 1/100 s at a rate of 5 frames/s. Kodak Plus-X Pan film (Eastman Kodak, Rochester, N.Y.) was used and processed following the conventional method. The screen was set at a 248-mm distance from the muscle fiber in early experiments. But, since we could not resolve sufficiently the microstructural elements in the first-order diffraction line with this setup, the screen was reset at a 833-mm distance from the fiber to enlarge the pattern. Both zero- and first-order lines were recorded in early experiments, whereas only the central region of the first-order line was recorded in later experiments.

Film Analysis

The film was analyzed in the following manner with a specially built microdensitometer. The diffraction lines on the film were magnified with a lens, and a photodiode was set at the plane of the image at the center of the optical axis. The aperture of the photodiode corresponded to 0.23 mm on the film, or ~12 nm difference in SL at SL ~3.0 μm. The film was moved with a motor at a speed of 0.34 mm/s, so that the photodiode crossed the diffraction lines perpendicularly, the position of the film being sensed with a potentiometer. The outputs of the potentiometer and the photodiode were fed to the X- and Y-axis of the X-Y recorder, respectively. We could resolve two parallel lines separated by 2-nm SL if the lines were sharp enough.

The sensitivity of the setup to the position of the diffraction line was checked using calibrated parallel lines. Spacing of the parallel lines could be measured with a precision equivalent to or better than 0.2-nm SL.

Computation of the SL Difference

Measuring the distance of individual microstructural elements from the zero-order line, we computed the SL from the Bragg equation, $d \sin \theta_n =$

Dr. Ishide's present address is First Department of Internal Medicine, Tohoku University School of Medicine, Sendai 980, Japan.

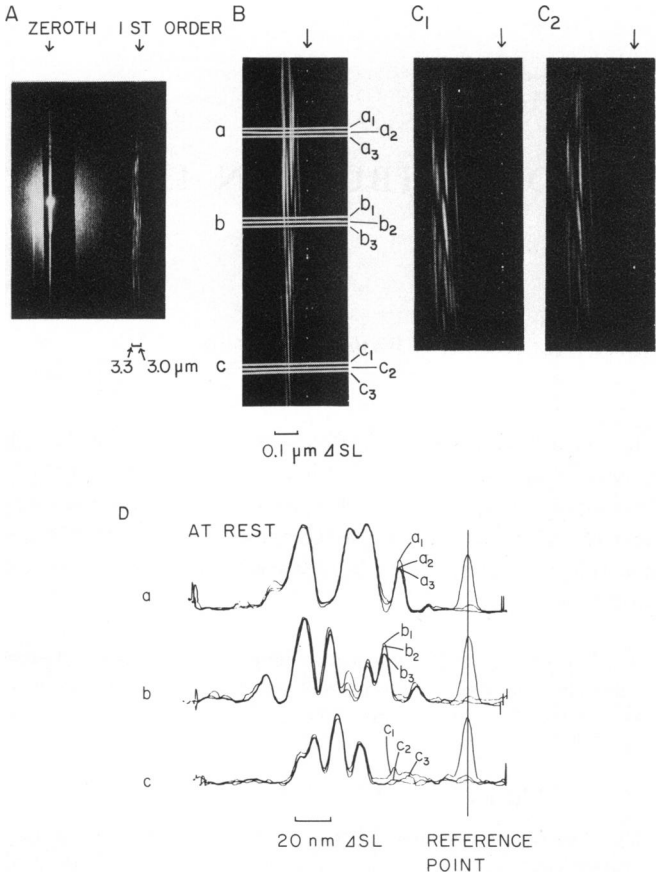

FIGURE 1 Examples of diffraction patterns (*A, B, C*) and microdensitometric trace (*D*). *A*, first-order diffraction pattern on one side of partially masked zero-order line in resting fiber with the screen at a 248 mm distance from fiber. *B* and *C*, central regions of first-order diffraction patterns with screen at a 833 mm distance from fiber. *B*, just before the onset of contraction. C_1 and C_2, 1.0 and 1.4 s after the onset, respectively, but still during tetanic contraction. *B* and *C* were obtained from one and the same contraction. Note the resemblance of the diffraction pattern in C_1 and C_2. Dotted lines are reference lines (arrows). Mean SL is ~2.9 μm in *B* and 3.0 μm in *C*. In *D*, traces *a*, *b* and *c* were obtained by scanning the regions designated by the corresponding letters in *B* with microdensitometer. In each trace, scans were made triplicate by slightly changing the scanning region.

$n\lambda$, where d is SL, n is the order of the diffraction line, θ_n is the angle between the nth and zero-order lines, and λ the wavelength of the laser beam. Observations were made in the Fraunhofer region. Inasmuch as the wave front of the laser beam is effectively planar and the distance from the specimen to the screen is large enough both for the size of aperture (a cluster of sarcomeres) and for the curvature of the wave front of the diffracted beam to be neglected, the Fraunhofer diffraction condition is satisfied. In the computation of the SL, we neglected the effect of the Ringer solution in the chamber and the cover glass above it, through which the diffracted beams came into the air. The error introduced by neglecting these effects was calculated to be ~0.07% of absolute SL, or ~2 nm at SL ~3.0 μm. This error was, however, cancelled out when the difference in SL was measured.

The distance of the microstructural element from the zero-order line was measured as the sum of the distances between the zero-order line and a reference line (X_1), and between the reference line and the microstructural element (X_2; see Fig. 1 *B-D*). X_2 could be calculated from the densitometer trace with an accuracy of >0.01 mm on the screen, while X_1 could be measured with the accuracy of only 1 mm because of some difficulty in determining the exact position of the center of zero-order line. Such an inaccuracy in reading the X_1 value could introduce a large error in the computation of absolute SL, but <0.2 nm in the computation of the SL difference.

The first-order line has some intrinsic curvature. The deviation of the first-order line from straight line was calculated to reach 3 nm at maximum in terms of SL in each frame of the film. However, the effect of the intrinsic curvature was again cancelled in the computation of the SL difference.

The total error introduced by the above-mentioned factors, would therefore not exceed 0.5 nm in the computation of the SL difference.

Experimental Procedure

To minimize the internal shortening of the fiber on contraction, the fiber was stretched so that the mean SL fell in the range of 2.6–3.3 μm in the resting state. The first-order diffraction line on the screen was set parallel to a reference line. Then, the fiber was made to contract tetanically by applying pulses of <2 ms duration with supramaximal intensity at 30 Hz. The contraction, which lasted 2–3 s, was repeated at intervals of no less than 5 min. The diffraction lines were photographed from just before the onset of contraction through the completion of relaxation. Though the tetanic force was not monitored, we checked frequently during each experiment to see if the fiber showed an all-or-none type response to increasing stimulus intensity under the light microscope.

Data were obtained by changing the laser-illuminating region and by varying the fiber length. Frames that contained microstructural elements parallel to the reference line were selected to be analyzed with the microdensitometer. The selected frames were scanned in three to five regions along the first-order line; scanning was made in triplicate in each region by moving the film slightly (Fig. 1*D*); this procedure ensured against misreading of the position of a peak due to random noise of the film. If the diffraction lines were very skewed, the peaks in the three scans failed to superimpose. Such peaks were rejected. The SL corresponding to each peak was computed. The SL difference corresponding to the distance between adjacent peaks in the trace was then calculated.

RESULTS

Fig. 1*A-C* illustrates typical examples of the first-order diffraction pattern obtained with the screen 248 mm (*A*) and 833 mm (*B, C*) distant from the fiber. Both zero-and first-order lines are seen in Fig. 1*A*, but only the central region of the first-order line in Fig. 1*B-C*. The first-order line was in every case composed of a number of microstructural elements, as has been reported by Cleworth and Edman (1972).

On contraction, during early rapid internal shortening of the fiber, the pattern of the first-order line changed and the individual microstructural elements became blurred. Blurring of the elements might be due either to the movement of the elements during the exposure of the film or to a decrease of uniformity within single clusters of sarcomeres, or both; we could not test these by reducing the exposure time because of the limited intensity of the laser beam. A clear pattern later emerged in contraction. The pattern then generally remained the same from about 0.5 to 1.0 s after the onset of contraction through the cessation of stimulation (Fig. 1C_1, C_2). This indicates that there were neither rapid fluctuations of SL, nor slow shortening or lengthening of SL during the steady state of contraction. This result agrees very well with the reports of

Cleworth and Edman (1972) that microstructural elements in the first-order line did not change their positions by greater than 5 nm SL, and by Haskell and Carlson (1981) using the quasi-elastic light scattering technique that there was little rapid fluctuation of SL during tetanic contraction. After stimulation ceased, the diffraction pattern returned to the resting pattern similar to the original one, though the pathway was not simply the reverse of that observed during the onset of contraction.

We assume that an individual, microstructural element has a corresponding cluster of sarcomeres with a homogeneous SL (see Discussion). To examine the nature of the difference of SL in various clusters, SL corresponding to individual microstructural elements were computed from the traces of the microdensitometric scans. However, as described in the Methods, there was some difficulty in computing the absolute value of SL with high accuracy. Therefore, we measured the difference in SL corresponding to the difference in spacing of adjacent microstructural elements lying in parallel, thereby increasing the accuracy.

In early experiments, we used the setup with the screen at a 248-mm distance from the fiber, where the resolution of the SL difference was ~10 nm. The histogram of the distribution of the SL difference from the resting state had a peak ~40–50 nm with the distribution from 10 to 130 nm, in agreement with the preliminary reports (Iwazumi et al., 1977; Halpern, 1978). On the other hand, the histogram from the contracting fibers had a distribution ranging from 10 to 130 nm without any prominent peak.

During the course of the above experiments, we noticed that the microstructure that was recognized as a single peak on the trace was actually often composed of more than one element. To increase the resolution of the SL difference, the screen distance from the fiber was increased to 833 mm. With this setup, as shown in Fig. 1*B*, we could identify clearly the microstructural elements located with small separation. If two microstructural elements were located within 2–3 nm of each other in terms of SL difference, we could not identify the elements as two. However, once an element was identified, the location of its peak could be identified with a resolution of better than 0.5 nm.

Fig. 2*A* and *B* show the histograms of the distribution of the SL difference obtained with the 833-mm distant screen from the resting and contracting fibers, respectively. It is apparent that the histogram of the resting state has a sharp peak at 12–14 nm. The histogram of the contracting state also appears to have a peak at ~12–14 nm, though the peak is broad compared with that in the histogram of the resting state and may be influenced by a nearby, secondary peak. Taking account of the resolution of setup (<0.5 nm) and the breadth of the latter peak, the difference in the peak values between the two histograms may be insignificant.

Besides the main peak, both histograms appear to have

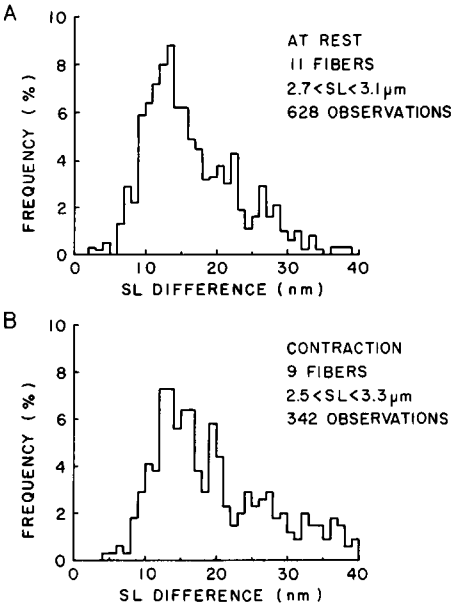

FIGURE 2 Histograms of the distribution of the SL difference obtained from resting (*A*) and contracting fibers (*B*) with the screen at a 833 mm distance from the fiber.

additional peaks; peaks at about 20–21 nm and at about 26–27 nm. The value of the latter peak is just twice the value of the main peak. However, further experimentation will be required to verify these additional peaks.

DISCUSSION

The first-order diffraction line from single muscle fibers of the frog consists of a number of microstructural elements. We found that the microstructural elements were separated from each other predominantly by a distance that corresponded to ~12–14 nm in terms of the SL difference. This suggests that the SL distribution is not continuous but discrete both during resting and contracting states, with the unit separation of SL about 12–14 nm. If the SL distribution were continuous, we would expect either a monotonic histogram without a prominent peak, or no microstructural elements at all in the diffraction pattern.

However, there are several possible alternative causes of the microstructure. They are (*a*) modulation of first-order diffraction line by some internal structure in the fiber; (*b*) modulation by the aperture function of the laser beam; (*c*) speckle effect of the laser beam; (*d*) multiple reflection of the diffracted beam by the cover glass; (*e*) diffraction from clusters of sarcomeres, which have the same SL but are located separately within the laser-illuminating region of the fiber; and (*f*) the Bragg angle effect. We thought these possibilities unlikely for the following reasons:

(*a*) Intervals of the structure that might modulate the first-order line were calculated to be >0.5 mm in the fiber. Such structure has not been reported nor could it be found under the light microscope.

(*b*) Since the intensity distribution of the laser beam is

gaussian, the Fourier transform of the intensity distribution contains no higher order lobes. This makes the second possibility improbable.

(*c*) The speckle effect occurs when a highly coherent light such as a laser beam is reflected by a rough surface. The granular nature of the background scattering around the zero-order beam appears to be due to the speckle effect. Since the size of individual granules was much smaller than the microstructural element, the microstructure may not be due to the speckle effect.

(*d*) Consider that the beam diffracted by the fiber hits a cover glass with the incident angle θ. The beam is partially reflected and partially transmitted at the first surface of the cover glass. The transmitted part is subsequently reflected back and forth between the two surfaces. The interval of the adjacent transmitted beams is given geometrically by $2D \tan \theta$ on the screen, where D is the thickness of the cover glass. Since $\tan \theta = 0.221$ at SL ~ 3.0 μm and $D = 0.17$ mm, the interval should be 0.07 mm, which corresponds to 1 nm difference in SL. This value is much smaller than the observed SL difference.

(*e*) It is possible that the beams diffracted by the separated clusters with the same SL go on in parallel, giving rise to the microstructural elements located closely to each other. We checked this by varying the distance of the screen from the fiber. The spacing of the microstructural elements varied as expected from the Bragg equation.

(*f*) Suppose that microstructural elements are entirely due to the Bragg angle effect. It follows that 12–14 nm separation of SL corresponds to the difference of ~0.001 rad in the skew angle of striation between the two corresponding clusters of sarcomeres; the dispersion of the striation skew angle within each cluster would have to be considerably <0.001 rad (0.057°). It is unclear why a region large enough to give an intense microstructural line should take on so precise an angle. Furthermore, to explain the observed shape of the histogram by the Bragg angle effect with a continuous SL distribution, it is necessary to assume a series of regular, discrete angles of striation skew. It would be surprising if the striation skew angles took on only such highly specific discrete values. Therefore, we believe that, though some microstructure may be due to the Bragg angle effect, the microstructure is predominantly due to the discrete nature of the SL distribution.

Consequently it is likely that the microstructure is due to the discrete nature of the SL distribution among clusters of sarcomeres. A rigorous theoretical justification is given in the accompanying paper by Judy et al. (1982).

A striking observation in the majority of fibers was that the microstructural pattern persisted virtually unchanged throughout the tetanic plateau. A similar persistence is evident in the records of Cleworth and Edman (1972). This stability implies that the sarcomere length distribution pattern in the field of view of the laser remained essentially fixed, for even slight distributional changes, such as those brought about by modest translation of the fiber across the laser beam, cause the microstructural pattern to be drastically altered. It appears that each sarcomere remains "locked" into a particular, well-defined, discrete length so long as the steady state of contraction persists.

Finally, the discrete, stable distribution observed here may be related to the stepwise shortening phenomenon reported earlier. Using laser diffraction (Pollack et al., 1977; 1979), and more recently direct imaging of striations (Delay et al., 1981; Jacobson et al., 1981) we have observed that sarcomeres shorten in a cascade of steps, with periods of "pause" interspersed between each step. These pause periods apppear to be quasi-stable states in which little or no SL change takes place, as above. If a shortening step from one to another pause state represents a shortening from one to another discrete sarcomere length, then the predominant size of the shortening step should be equal to the predominant SL difference reported here. The two values of 11–12 nm (Jacobson, et al., 1981) and 12–14 nm, respectively, are close enough to suggest that this may be the case.

This work was supported in part by grant HL 18676 from the National Institutes of Health, and grants from the American Heart Association and Muscular Dystrophy Association

Received for publication 5 June 1981 and in revised form 23 September 1981.

REFERENCES

Clewoth, D.R., and K.A.P. Edman. 1972. Changes in sarcomere length during isometric tension development in frog skeletal muscle. *J. Physiol. (Lond.).* 227:1–17.

Delay, M.J., N. Ishide, R.C. Jacobson, G.H. Pollack, and R. Tirosh. 1981. Stepwise sarcomere shortening: analysis by high-speed cinematography. *Science (Wash., D.C.)* 213:1523–1525.

Halpern, W. 1978. Distribution of 1st order diffraction line peaks obtained from frog skeletal muscle. *Biophys. J. (Abstr.).* 21:56*a*.

Haskell, R.C., and F.D. Carlson. 1981. Quasi-elastic light-scattering studies on single skeletal muscle fibers. *Biophys. J.* 33:39–62.

Iwazumi, T., H.E.D.J. Ter Keurs, and G.H. Pollack. 1977. Do sarcomeres assume discrete lengths? *Biophys. J. (Abstr.).* 17:199*a*.

Jacobson, R.C., R. Tirosh, M.J. Delay, and G.H. Pollack. 1981. Real time high speed sarcomere length measurements from optical image. *Biophys. J. (Abstr.).* 33:223*a*.

Judy, M.M., V. Summerour, T. LeConey, and G.H. Templeton. 1982. Muscle diffraction theory: the effects of aberrations in the spatial regularity of a three-dimensional sarcomere array. *Biophys. J.* 37:475–487.

Pollack, G.H., T. Iwazumi, H.E.D.J. Ter Keurs, and E. Shibata. 1977. Sarcomere shortening in striated muscle occurs in stepwise fashion. *Nature (Lond.).* 268:757–759.

Pollack, G.H., D.V. Vassallo, R.C. Jacobson, T. Iwazumi, and M.J. Delay. 1979. Discrete nature of sarcomere shortening in striated muscle. *In* Cross-bridge Mechanisms in Muscle Contraction. H. Sugi and G.H. Pollack, editors. University Park Press, Baltimore, Md. 23–40.

Rüdel, R., and F. Zite-Ferenczy. 1979. Do laser diffraction studies on striated muscle indicate stepwise sarcomere shortening? *Nature (Lond.). 278:573–575.*